

Iragi National Journal of Earth Science



www.earth.mosuljournals.com

Mapping of Rock Vulnerability in Rantepao City, Indonesia for Disaster Mitigation Based on Microtremor Data

Alexander Pakiding 1* D, Adi Maulana 2 D, Busthan Azikin³ D

Article information

Received: 23-Jun-2024
Revised: 25-Jul-2024

Accepted: 31-Aug-2024

Available online: 01-Oct-2025

Keywords:

Mapping

Rock susceptibility Disaster mitigation Microtremor

Correspondence:

Name: Alexander Pakiding

Email: alexpakiding1@gmail.com

ABSTRACT

Rantepao City is the capital of North Toraja Regency. In recent years, the development in this city has been quite rapid; many high-rise buildings have begun to be built in both form of residential and office. Based on the 2019 Map of Indonesia's Disbursement Vulnerability Zone, Rantepao City is in a moderate liquefaction zone. Therefore, it is considered necessary to research to map Rock Vulnerability using Microtremor data. This research is quantitative. Measurements are taken at 13 points with a duration of 45 minutes. The tools needed in data collection are a set of microtremors to record microwaves, and a GPS to find out the coordinates of the measurement points. From the results of microtremor measurements in the city of Rantepao, each region has variable frequency values (F0) ranging from 0.470853 to 14.6016, amplification values (A0) ranging from 2.86703 to 8.39741, and a susceptibility index (Kg) ranging from 1.146179 to 24.87313. This indicates that the constituent rocks vary from hard to soft alluvial deposits. The lower the F0, the thicker the sediment layer is above the bedrock. Hard alluvial deposits tend to have a lower amplification factor compared to soft alluvial deposits. Based on the amplification factor, the hard alluvial deposits have lower values compared to soft alluvial deposits. With this map, it is hoped that the community can find out the condition of the rocks where they live and become a reference for the government in regional development planning.

DOI: 10.33899/earth.2024.150972.1304, ©Authors, 2025, College of Science, University of Mosul. This is an open-access article under the CC BY 4.0 license (http://creativecommons.org/licenses/by/4.0//).

¹ Universitas Hasanuddin

^{2,3} Earth and Environmental Technology Study Program, Faculty of Engineering, Hasanuddin University, Makassar, Indonesia.

رسم خرائط هشاشة الصخور في مدينة رانتيباو، إندونيسيا، للتخفيف من آثار الكوارث بناءً على بيانات الهزات الدقيقة

ألكسندر باكيدينغ 1° 🕞، آدي مولانا 2 🕞، بوستان أزيكين 3

¹ جامعة حسن الدين.

3.2 برنامج دراسة تكنولوجيا الأرض والبيئة، كلية الهندسة، جامعة حسن الدين، ماكاسار، إندونيسيا.

الملخص

مدينة رانتيباو هي عاصمة مقاطعة شمال توراجا. شهدت المدينة في السنوات الأخيرة تطورًا سربعًا؛ حيث بدأ تشييد العديد من المباني الشاهقة، سواءً السكنية أو المكتبية. واستنادًا إلى خربطة منطقة الهشاشة في إندونيسيا لعام 2019، تقع مدينة رانتيباو في منطقة تمييع معتدلة. لذلك، يُعدّ البحث في رسم خرائط هشاشة الصخور باستخدام بيانات الهزات الدقيقة أمرًا ضروريًا. هذا البحث كمي، حيث أُخذت القياسات في 13 نقطة بمدة 45 دقيقة. الأدوات اللازمة لجمع البيانات هي مجموعة من أجهزة قياس الاهتزازات الدقيقة لتسجيل الموجات الدقيقة، ونظام تحديد المواقع العالمي (GPS) لتحديد إحداثيات نقاط القياس. بناءً على نتائج قياسات الاهتزازات الدقيقة في مدينة رانتيباو، لكل منطقة قيم تردد متغيرة (FO) تتراوح من 0.470853 إلى 14.6016، وقيم تضخيم (A0) تتراوح من 2.86703 إلى 8.39741 إلى 24.87313. يشير (Kg) تتراوح من 1.146179 إلى 24.87313. يشير هذا إلى أن الصخور المكونة تتراوح من رواسب طينية صلبة إلى رواسب طينية لينة. كلما انخفض مؤشر FO ، زادت سماكة طبقة الرواسب فوق الصخر الأساسي. تميل الرواسب الطميية الصلبة إلى أن يكون لها عامل تضخيم أقل مقارنةً بالرواسب الطميية اللينة. بناءً على عامل التضخيم، تكون الرواسب الطميية الصلبة ذات قيم أقل مقارنة بالرواسب الطميية اللينة. من خلال هذه الخريطة، يُؤمل أن يتمكن المجتمع من معرفة حالة الصخور في مناطق سكنه، وأن يصبح مرجعًا للحكومة في تخطيط التنمية الإقليمية.

معلومات الارشفة

تاربخ الاستلام: 23-يونيو -2024

تاريخ المراجعة: 25-يوليو -2024

تاريخ القبول: 31- أغسطس-2024

تاريخ النشر الالكتروني: 01- اكتوبر -2025 الكلمات المفتاحية:

رسم الخرائط

قابلية الصخور للتأثر

التخفيف من آثار الكوارث

الزلزال الدقيق المراسلة:

الاسم: ألكسندر باكيدينغ

Email: alexpakiding1@gmail.com

DOI: 10.33899/earth.2024.150972.1304, ©Authors, 2025, College of Science, University of Mosul. This is an open-access article under the CC BY 4.0 license (http://creativecommons.org/licenses/by/4.0/).

Introduction

The Indonesian archipelago is located at the meeting point of three major tectonic plates: the Eurasian, Pacific, and Indo-Australian. This convergence of plates has significant implications for the region. The subduction of the Indo-Australian Plate beneath the Eurasian Plate and the Pacific Plate has resulted in the formation of the Sunda Arc, which includes active volcanoes and is prone to earthquakes (Yamada *et al.*, 2021). The subduction zone along the Sunda Trench has produced several significant earthquakes, including the devastating 2004 Indian Ocean earthquake and tsunami (Uchida *et al.*, 2020). The collision between the Indo-Australian and Eurasian Plates has also led to uplifting mountain ranges, such as the Himalayas and the Indonesian mountains (Sunaryo, Mala and Prasetio, 2018). These tectonic processes contribute to the Indonesian archipelago's high seismic activity and volcanic eruptions, making it a region of significant geo-hazards (Yanti *et al.*, 2020; Asnawi *et al.*, 2022).

The earthquake in Sulawesi, Indonesia, in September 2018 had significant impacts. It triggered liquefaction and tsunamis, causing severe damage and casualties (Maly and Suppasri, 2020). The tsunami waves reached heights of up to 10.7 meters in some areas and inundation distances of up to 488 meters (Sassa and Takagawa, 2019). The run-up height and inundation were observed in 18 selected sites, mainly in Palu Bay (Tunas et al., 2020). The damage to

buildings and infrastructure was categorized into three types: earthquake damage, liquefaction damage, and tsunami damage (Widiyanto *et al.*, 2019). Earthquake damage included horizontal collapse, cracking, and fractured structures, while liquefaction damage involved objects and buildings being turned over, rotated, or sunk in water or mud (Elbanna *et al.*, 2021). Tsunami damage was characterized by objects, buildings, or structures being washed away from the shoreline. The impacts of the tsunami were most severe within 150 meters of the coastline.

Microtremor data can be used to measure rock susceptibility. The paper "Context_5" discusses the application of microtremor array measurement (MAM) as a non-invasive surface wave survey for mapping soil/rock interfaces. The study conducted in Singapore used MAM tests to identify the depth of rock interfaces in different geological formations. The results showed that a standard shear wave velocity (Vs) of 500 m/s was suitable for interpreting the soil/rock interface in the Bukit Timah Granite and Jurong formations. However, the method did not predict well for soft Kallang Formation deposits. The paper "Context_3" also mentions using microseismic (MS) monitoring data, including MS raw wave data and MS energy data, to predict high-energy tremors and rockburst risk. Support vector machine (SVM) and genetic algorithm (GA) were used to analyze the MS data and classify high-energy tremors. Therefore, microtremor data can be utilized to measure rock susceptibility and predict rockburst risk (Cao et al., 2020; Qu et al., 2020).

The seismic hazard mapping based on the shear strain indicator was conducted in Bengkulu City, Indonesia (Farid and Mase, 2020). The study aimed to assess the possible damage that could occur in the area and provide recommendations for seismic hazard mitigation. The values of ground shear strain were used as indicators for potential damage, and microtremor measurements were performed to obtain the geophysical description of the study area. The horizontal-to-vertical spectral ratio (H/V) analysis was conducted to determine peak amplitude and predominant frequency, which were then used to calculate vulnerability indices and ground shear strain. The results showed that Bengkulu City was generally vulnerable to seismic impact, with a particular focus on the coastal area due to the potential for liquefaction damage. The study provided valuable information for stakeholders to consider in their seismic hazard mitigation efforts.

This research is conducted to make a map of rock vulnerability in Rantepao City with the aim of disaster mitigation and becoming a reference for the community and the government in development planning.

Materials And Methods

This research was conducted in Rantepao City, North Toraja Regency, South Sulawesi Province, Indonesia. This is a quantitative study, namely by taking measurements at 13 points with a duration of 45 minutes. The tools needed in data collection are a set of microtremor tools to record microwaves, and a GPS to find out the coordinates of the measurement point. The resulting data is stored on a computer hard drive and then processed using Geopsy software to obtain the dominant frequency value F0, and the amplification value A0 is then used to calculate the value of the rock susceptibility index Kg. Low Kg value (Kg < 6) indicates that the area is resistant to earthquake shocks, and conversely, areas with high Kg (Kg > 6) are vulnerable or not strong enough to withstand vibrations. This value provides an overview of the physical properties of rocks in the research area. Surface software is used to create a map of the rock vulnerability index so that the way they are distributed in the study area can be explained.

Results

Measurement Location

Microtremor measurements in Rantepao City are carried out at thirteen points. The coordinates of the location of the measurement points are shown in Table 1.

Measurement Points	Long.	Lat.	Location	Elevation (m)
1	119.8989778	-2.974588889	S Parman Street	783
2	119.8963056	-2.972072222	Bakti Court	781
3	119.9080083	-2.970163889	Near SMK Nusantara	822
4	119.9098694	-2.967130556	SMK TagariRantepao	788
5	119.9119917	-2.960775	Front of Tedong Rantepao Market	791
6	119.9121972	-2.954	Front of Tallunglipu residents' houses	803
7	119.9232194	-2.954222222	Behind Campus 2 UKI Toraja	824
8	119.9052056	-2.965719444	Tagari Street Near SMA Pelita	791
9	119.9048944	-2.958822222	Rear Catholic Church- Agata Stasi Tallunglipu South	832
10	119.8944944	-2.964794444	Tongkonan Bamba	784
11	119.8896583	-2.960027778	Kondongan	792
12	119.8949	-2.958013889	Lembah Keramat	786
13	119.9157389	-2.956880556	Pawnshop Street	797

Table 1: Coordinates of the location of measurement points and their elevation.

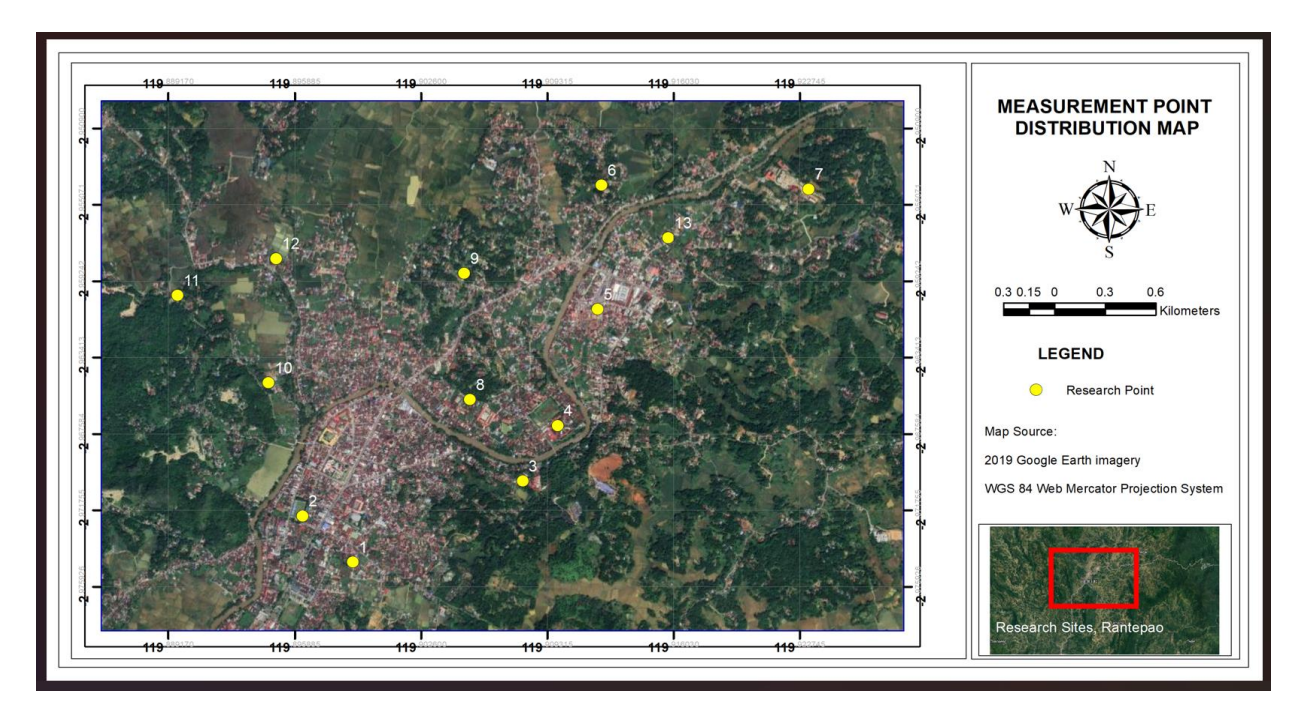


Fig. 1. Position on the map of the 13 measurement points in Rantepao City.

Measurement Results

Microseismic signals recorded in signal form were lagged using Geopsy software, and the obtained data are exhibited in Table 2 below. The values of A0 and F0 are obtained from the results of data processing, as shown in Figure 2, namely, the recording at measurement point 3.

Table 2: Measurement Results.

Measuring Point	Location	T dom (s)	A0 (μm)	F0 (Hz)	Kg (Cal)
1	S Parman Street	0.104443	4.52188	9.57457	2.135594
2	Bakti Court	0.083763	5.40122	11.9385	2.443622
3	Near SMK Nusantara	0.282408	4.41442	3.54098	5.503308
4	SMK TagariRantepao	0.108618	3.24844	9.20656	1.146179
5	Front of Tedong Rantepao Market	0.115065	3.2221	8.69076	1.194594
6	Front of Tallunglipu residents' houses	0.344312	2.86703	2.90434	2.830199

7	Behind Campus 2 UKI Toraja	0.209521	8.39741	4.77279	14.77469
8	Tagari Street Near SMA Pelita	0.125309	3.48165	7.98029	1.518978
9	Rear Catholic Church- Agata Stasi Tallunglipu South	0.254537	3.02503	3.9287	2.32922
10	Tongkonan Bamba	0.093415	7.90389	10.7049	5.835783
11	Kondongan	0.068486	4.81978	14.6016	1.590941
12	Lembah Keramat	0.112426	3.00464	8.89473	1.014967
13	Pawnshop Street	2.123805	3.42222	0.470853	24.87313

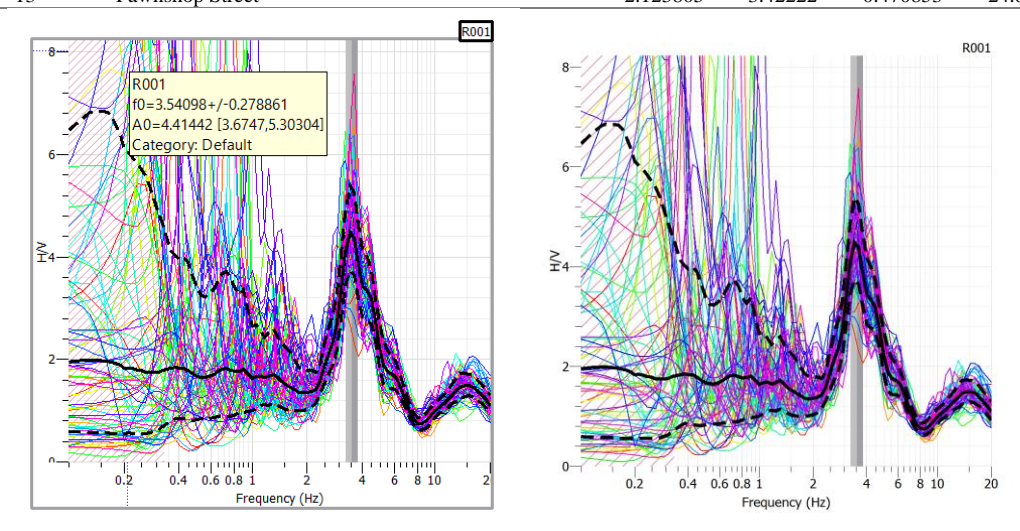


Fig. 2. Amplification of the study area at measurement (point 3).

Discussion

Dominant Period (T_{dom}).

The dominant period of microtremor measurement refers to the characteristic frequency at which the microtremor signal has the highest amplitude. It is an important parameter in assessing the dynamic nature of an area and understanding its response to seismic waves. The dominant period can be estimated by analyzing the horizontal-to-vertical spectral ratio (HVSR) from microtremor data. The HVSR method involves measuring the horizontal and vertical components of the microtremor signal and calculating the ratio between their spectral amplitudes. By identifying peak frequencies in the HVSR curve, dominant periods can be determined. This information is invaluable for seismic hazard assessment and site-specific structure design (Khalili and Mirzakurdeh, 2019; Farid and Mase, 2020).

The Dominant Period (Tdom) measurement is intended to reveal the characteristics of rocks at a specific location. The characteristics are grouped based on Zhao's classification in 2006, as shown in the following table (3):

Table 3: Zhao's classification in 2006 (Yang et al., 2017).

Type	Classification	
(Rock - T0 < 0.2 s)	SA+SB	
(Hard Soil - $0.2 \le T0 < 0.4 \text{ s}$)	SC	
(Medium Soil - $0.4 \le T0 < 0.6 \text{ s}$)	SD	
(Soft Soil - $T0 \ge 0.6 \text{ s}$)	SE	

SA = Hard Rock, SB = Rock, SC = Hard Soil, SD = medium Soil, SE = soft Soil.

SA + SB = hard rocks and ordinary rocks (Rock)

Based on Zhao's classification in Table 3 and Table 2 column 3, the results at 13 measurement points are shown in Table 4.

Based on Table (4) above, the T_{dom} value ranges from 0.068486 s - 2.123805 s. Measurement point 13 is the area that has the highest T_{dom} value and is included in the SE category in the form of soft soil. Point 13 is adjacent to point 5, and about 20 years ago, it was a rice field area only because the area of point 5 is now a market location, so the surrounding land has become dense. Point 11 is an area that has the lowest T_{dom} value and is included in the SA + SB category in the form of rocks.

Table 4: Dominant period and category of rocks.

Measuring Point	Location	T _{dom} (s)	Soil Type	Category
1	S Parman Street	0.104443	SA + SB	Rock
2	Bakti Court	0.083763	SA + SB	Rock
3	Near SMK Nusantara	0.282408	SC	Hard Soil
4	SMK Tagari Rantepao	0.108618	SA + SB	Rock
5	Front of Tedong Rantepao Market	0.115065	SA + SB	Rock
6	Front of Tallunglipu residents' houses	0.344312	SC	Hard Soil
7	Behind Campus 2 UKI Toraja	0.209521	SC	Hard Soil
8	Tagari Street Near SMA Pelita	0.125309	SA + SB	Rock
9	Rear Catholic Church- Agata Stasi Tallunglipu South	0.254537	SC	Hard Soil
10	Tongkonan Bamba	0.093415	SA + SB	Rock
11	Kondongan	0.068486	SA + SB	Rock
12	Lembah Keramat	0.112426	SA + SB	Rock
13	Pawnshop Street	2.123805	SE	Soft Soil

Amplification Factor (A0)

Variations influence the amplification factor value in geological formations, thickness, and physical properties of soil and rock layers, depth of bedrock and underground water surface, and surface of subsurface structures. The amplification factor describes the magnitude of wave reinforcement when passing through a medium (Oliveira et. al., 2006; in Kusumaputra, 2012).

The amplification factor A0 value is obtained from data processing using Geopsy software, which is like to Figure (2) above, and the A0 value at 13 measurement points is in Table (2 column 4). The A0 value obtained has a range value from 2.86-8.39. Based on this value, four zones of amplification factors are obtained according to the classification of Setiawan (2009). Where a low category value (amplification value < 3) indicates that the area is a solid geological unit. The medium category of amplification values ($3 \le A0 < 6$) indicates that the measurement point is in a less dense geological unit area. High category with amplification values of $6 \le A0 < 9$, and very high if $A0 \ge 9$. (Demulawa and dan Druwati, 2021)

Table 5: Classification of Amplification Factor Values (Demulawa, M., dan Druwati, 2021)

Zone	Value of the Amplification Factor	Classification
1	A0 < 3	Low
2	$3 \le A0 < 6$	Medium
3	$6 \le A0 < 9$	High
4	A0 ≥ 9	Very High

Based on the classification in Table 5, the results of categorization are obtained at 13 measurement points in Table 6 as follows:

Table 6: Amplification Factor and Category measured at 13 different locations.

Measurement Poin	t Location	A0	Category
1	S. Parman Street	4.52188	Medium
2	Bakti Court	5.40122	Medium
3	Near SMA Nusantara	4.41442	Medium
4	SMK Tagari Rantepao	3.24844	Medium
5	Front of Tedong Market Rantepao	3.2221	Medium
6	Front of the house residents of Tallunglipu	2.86703	Low
7	Behind Campus 2 UKI Toraja	8.39741	High
8	Tagari Street Near SMA Pelita	3.48165	Medium
9	Behind Sta. Agata Catholic Church South Tallunglipu	3.02503	Medium
10	Tongkonan Bamba	7.90389	High
11	Kondongan	4.81978	Medium
12	Lembah Keramat	3.00464	Medium
13	Pawnshop Street	3.42222	Medium

The results of measuring the amplification value at the 13 measuring points (Table 6) above, the value ranges from 2.86703 to 8.39741. It is divided into three categories, namely 1 point with the low category, 10 points with the medium category, and 2 points with the high category. Two locations of measuring points, namely in the Tongkonan Bamba area (point 10) and in the area around campus 2 Kakondongan (point 7), are areas with high amplification factors.

Frekuensi Natural (F0)

The natural frequency (F0), also known as eigenfrequency, is the oscillating frequency that a system tends to have when it is allowed to vibrate without damping or excitation. In soil vulnerability analysis, the F0 value is closely related to the geological condition of the study area. Areas with characteristics of hard rocks and thin sediments have a high natural frequency, softer rocks with large sediment thickness, while soft rocks with high sediment thickness have a low natural frequency (Demulawa and dan Druwati, 2021). If it is associated with liquefaction, then softer rocks such as alluvial deposits or clay tend to have lower frictional strength, which makes them more susceptible to liquefaction when exposed to seismic shocks. The thickness of the sediment layer also plays an important role in the liquefaction potential. The thicker the sediment layer, the greater the volume of water trapped between the sediment particles. When a shock occurs, the pore water pressure increases and can exceed the frictional force between the particles, causing the soil to behave like a liquid.

From the results of measurements at 13 points, the value of F0 is obtained as in Table 2 column 5, where the value ranges from 0.470853 to 14.6016. The lowest F0 value is at point 13, which indicates that this area has soft rock characteristics. Areas whose conditions include this category are at points 3, 6, 7, and 9. This area is a rice field area where some have begun to build residential houses, but there is still a lot of water seeping between the existing buildings. Meanwhile, the measurement location of point 11 is the area with the highest F0 value, which indicates that the area has hard characteristics. This is following field observations, where this area is located at the edge of a mountain and is at a settlement, where the naked eye can see large stones exposed on the surface.

Seismic Susceptibility Index (Kg)

The Seismic Susceptibility Index (Kg) is a number that shows the level of vulnerability to earthquakes based on the condition of the rocks in the area. This seismic vulnerability, the value is different in each region. The reference of the Kg number is usually compared to other points in the area. After obtaining the value of the Dominant Period (T_{dom}) and the Amplific factor then look for the Seismic Vulnerability Index (Kg) using the formula: $Kg = A0^2 \div F0$ (Widyawarman and Fauzi, 2020).

Table 7: Seismic vulnerability index value classification (Refrizon, 2013).

Zone	Kg Value
Low	< 3
Medium	3 - 6
High	> 6

Using the Kg formula and the classification in Table 7, the Kg value and its category are obtained in the following Table 8.

The vulnerability index is shown in the map in Figure 3 above. The light color indicates a small vulnerability index value, and dark indicates a larger vulnerability index value. With the map, it can be seen how the distribution of rock vulnerability at the research site. More vulnerable areas behind Campus 2 UKI Toraja are located in the upper right corner in figure (3 or point 7). The area near SMA Nusantara (point 3) and Tongkonan Bamba (point 10) is an area with moderate vulnerability and has a slightly dark color.

Figure 4 is a geological map that is overlaid with a vulnerability index map. If you observe the geological map, the rocks at the research site can be grouped into only two parts, namely blue rocks composed of Nummulitic limestone and recrystallized limestone, partly and Sheared and green rocks composed of alternating quartz sandstone, shale and silt with intercalation of quartz conglomerates, carbon claystone, limestone, marl, green sandstone, calcareous sandstone and coal, locally with a thin layer of resin in the clay. However, because this area has developed into a region where some of these locations have been treated both by hoarding and due to other activities, which result in changes in both the thickness and hardness of the rocks.

This results in measurement results using microtremors that are different from geological map images. Because the microtremor data collection was carried out in 2023, while the geological map used was from 2010, the level of accuracy is higher. Especially based on field observations, when taking measurements, it is also closer to the results of microtremor measurements.

Table 8: 1	Kg values and	categories at 13	measurement points.
------------	---------------	------------------	---------------------

Measuring Point	Location	F0	A0	Kg	Category
1	S Parman Street	9.57457	4.52188	2.135594	Low
2	Bakti Court	11.9385	5.40122	2.443622	Low
3	Near SMK Nusantara	3.54098	4.41442	5.503308	Medium
4	SMK TagariRantepao	9.20656	3.24844	1.146179	Low
5	Front of Tedong Rantepao Market	8.69076	3.2221	1.194594	Low
6	Front of Tallunglipu residents' houses	2.90434	2.86703	2.830199	Low
7	Behind Campus 2 UKI Toraja	4.77279	8.39741	14.77469	High
8	Tagari Street Near SMA Pelita	7.98029	3.48165	1.518978	Low
9	Rear Catholic Church- Agata Stasi Tallunglipu South	3.9287	3.02503	2.32922	Low
10	Tongkonan Bamba	10.7049	7.90389	5.835783	Medium
11	Kondongan	14.6016	4.81978	1.590941	Low
12	Lembah Keramat	8.89473	3.00464	1.014967	Low
13	Pawnshop Street	0.470853	3.42222	24.87313	High

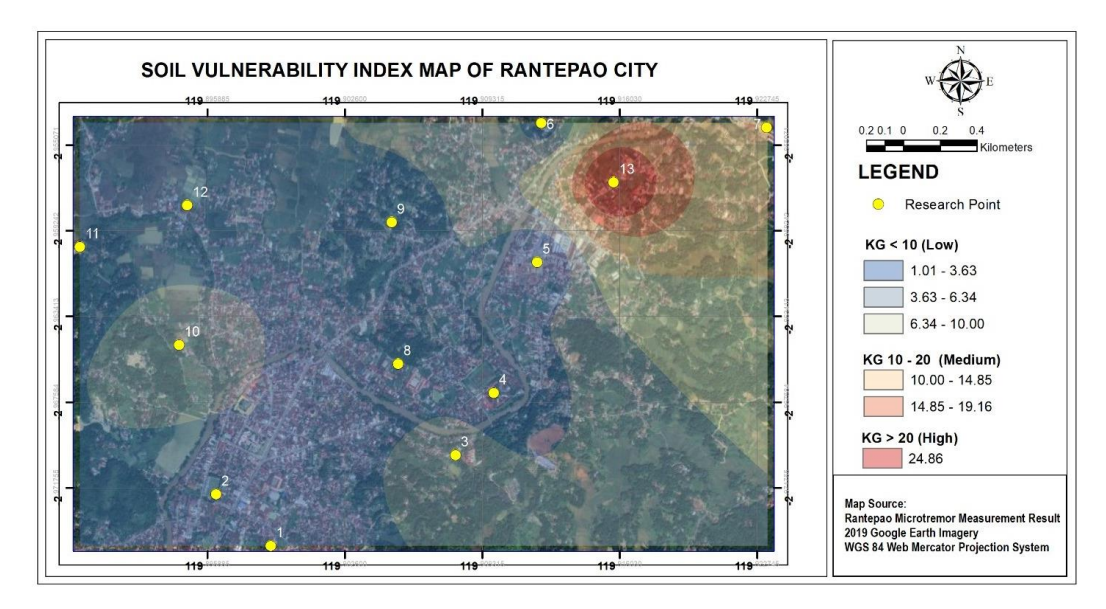


Fig. 3. Soil Vulnerability Index Map of Rantepao City

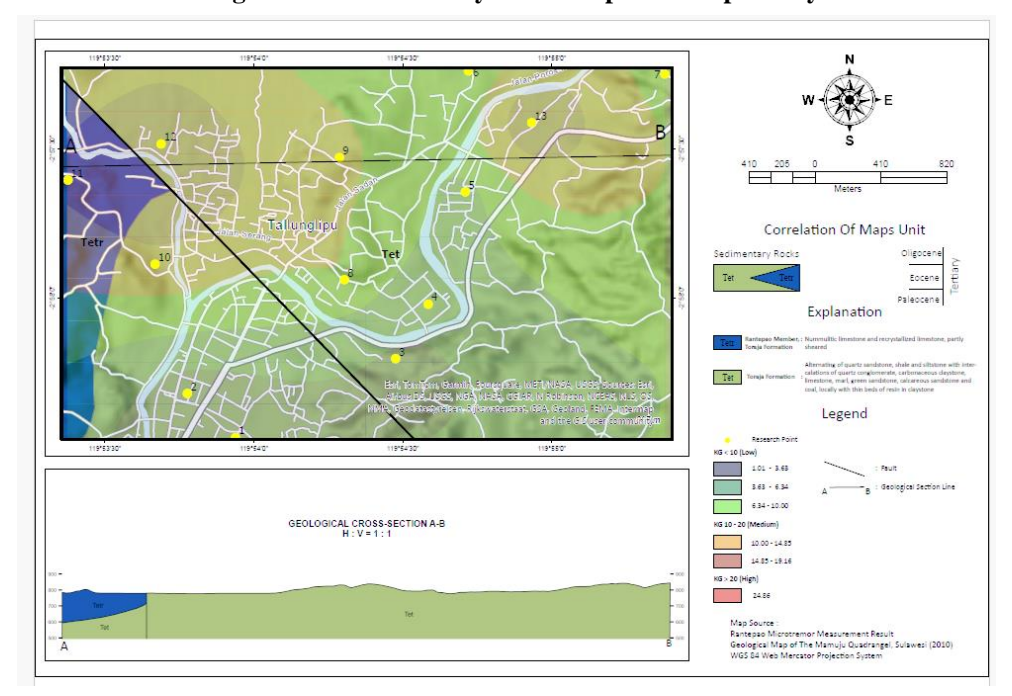


Fig. 4. Geological map in overlay with rock vulnerability index map.

Conclusion

From the results of microtremor measurements in the city of Rantepao, it is known that each region has a variable seismic vulnerability index value. The range of seismic vulnerability values in the city of Rantepao ranges from 1.146179 - 24.87313, which shows that the constituent rocks vary from hard to soft alluvial deposits. The map of the vulnerability index of rocks in the city of Rantepao (Fig. 3) shows how the distribution of rock hardness levels is. With the map in Figure 3, the condition of the rocks in the area can be known and can be a guide for planning land use, both by the local community and by the local government. Based on the F0 value, the thickest and softest layer of sediment is at measurement point 13, and the thinnest and hardest layer is at measurement point 11. The difference in layer hardness is expressed by the value of A0, where the area with the lowest difference is at measurement point 6 and the highest is at measurement point 7.

Acknowledgment

We would like to thank the UKI Toraja Leadership, the Head of BMKG Region IV, and Mr. Jamroni Tews, Mr. Kaharuddin, and Mr Karnaen for their assistance with funds, equipment, and support.

Conflict of Interest

The author hereby declares that the publication of this manuscript has no conflict of interest.

References

- Asnawi, Y, Simanjuntak, A., Muksin, U., Rizal, S., Syukri, M.S.M., Maisura, M., and Rahmati, R., 2022. Analysis of Microtremor H/V Spectral Ratio and Public Perception for Disaster Mitigation, International Journal of GEOMATE, 23(97), pp. 123–130. https://doi.org/10.21660/2022.97.3311.
- Cao, W., Durucan, S., Cai, W., Shi, J.Q., Korre, A., Jamnikar, S., Rošer, J., Lurka, A. and Siata, R., 2020. The role of mining intensity and pre-existing fracture attributes on spatial, temporal and magnitude characteristics of microseismicity in longwall coal mining. Rock Mechanics and Rock Engineering, 53(9), pp.4139-4162. https://doi.org/10.1007/s00603-020-02158-4.
- Demulawa, M., dan Druwati, I., 2021. Analisis Frekuensi Natural dan Potensi Amplifikasi Menggunakan Metode HVSR, Edu Research, 10(1), pp. 59–63.
- Elbanna, A., Abdelmeguid, M., Ma, X., Amlani, F., Bhat, H.S., Synolakis, C. and Rosakis, A.J., 2021. Anatomy of strike-slip fault tsunami genesis. Proceedings of the National Academy of Sciences, 118(19), p.e2025632118. https://doi.org/10.1073/pnas.2025632118.
- Farid, M. and Mase, L.Z., 2020. Implementation of seismic hazard mitigation on the basis of ground shear strain indicator for spatial plan of Bengkulu city, Indonesia, International Journal of GEOMATE, 18(69), pp. 199–207. https://doi.org/10.21660/2020.69.24759.
- Khalili, M. and Mirzakurdeh, A.V., 2019. Fault detection using microtremor data (HVSR-based approach) and electrical resistivity survey, Journal of Rock Mechanics and Geotechnical Engineering, 11(2), pp. 400–408. https://doi.org/10.1016/j.jrmge.2018.12.003.
- Maly, E. and Suppasri, A., 2020. The Sendai Framework for Disaster Risk Reduction at Five: Lessons from the 2011 Great East Japan Earthquake and Tsunami, International Journal of Disaster Risk Science, 11(2), pp. 167–178. https://doi.org/10.1007/s13753-020-00268-9.

- Qu, S., Guan, Z., Verschuur, E. and Chen, Y., 2020. Automatic high-resolution microseismic event detection via supervised machine learning. Geophysical Journal International, 222(3), pp.1881-1895. https://doi.org/10.1093/gji/ggaa193.
- Sassa, S. and Takagawa, T., 2019. Liquefied gravity flow-induced tsunami: first evidence and comparison from the 2018 Indonesia Sulawesi earthquake and tsunami disasters, Landslides, 16(1), pp. 195–200. https://doi.org/10.1007/s10346-018-1114-x.
- Sunaryo, Mala, H.U., and Prasetio, A., 2018. Earthquake microzonation study on Batubesi Dam of Nuha, East Luwu, South Sulawesi, Indonesia, International Journal of GEOMATE, 15(48), pp. 148–154. https://doi.org/10.21660/2018.48.40882.
- Tunas, I.G., Tanga, A., and Oktavia, S.R., 2020. Impact of landslides induced by the 2018 Palu earthquake on flash flood in Bangga River Basin, Sulawesi, Indonesia, Journal of Ecological Engineering, 21(2), pp. 190–200. https://doi.org/10.12911/22998993/116325.
- Uchida, N., Takagi, R., Asano, Y., and Obara, K., 2020. Migration of shallow and deep slow earthquakes toward the locked segment of the Nankai megathrust. Earth and Planetary Science Letters, 531, p.115986. https://doi.org/10.1016/j.epsl.2019.115986.
- Widiyanto, W., Santoso, P.B., Hsiao, S.C., and Imananta, R.T., 2019. Post-event field survey of 28 September 2018 Sulawesi earthquake and tsunami. Natural Hazards and Earth System Sciences, 19(12), pp.2781-2794. https://doi.org/10.5194/nhess-19-2781-2019.
- Widyawarman, D. and Fauzi, E.R., 2020. Microtremor Application for Microzonation of Earthquake Disaster Potential Levels at Campus I of PGRI Yogyakarta University, Journal Geosaintek, 6(2), p. 87-96. https://doi.org/10.12962/j25023659.v6i2.6778.
- Yamada, T., Kurokawa, A.K., Terada, A., Kanda, W., Ueda, H., Aoyama, H., Ohkura, T., Ogawa, Y. and Tanada, T., 2021. Locating hydrothermal fluid injection of the 2018 phreatic eruption at Kusatsu-Shirane volcano with volcanic tremor amplitude. Earth, Planets and Space, 73(1), pp. 1-15. https://doi.org/10.1186/s40623-020-01349-1.
- Yang, H., Lu, K. and Zhao, Y., 2017. A nonparametric approach for partial areas under ROC curves and ordinal dominance curves, Statistica Sinica, 27(1), pp. 357–371. https://doi.org/10.5705/ss.2013.367.
- Yanti, B., Mulyadi, E., Wahiduddin, R.G.H.N.Y. and Natalia Sri Martani, N., 2020. Community knowledge, attitudes, and behavior towards social distancing policy as a means of preventing transmission of COVID-19 in Indonesia. J Adm Kesehat Indones, 8(1), pp. 4-14. https://doi.org/10.20473/jaki.v8i2.2020.4-14.